Vacuum Rabi Splitting in a Semiconductor Circuit QED System

H. Toida,* T. Nakajima,† and S. Komiyama

Department of Basic Science, University of Tokyo, 3-8-1 Komaba, Meguro-ku, Tokyo 153-8902, Japan

(Received 22 June 2012; published 6 February 2013)

Vacuum Rabi splitting is demonstrated in a GaAs double quantum dot system coupled with a coplanar waveguide resonator. The coupling strength g, the decoherence rate of the quantum dot γ, and the decay rate of the resonator κ are derived, assuring distinct vacuum Rabi oscillation in a strong coupling regime [$(g, \gamma, \kappa) \approx (30, 25, 8.0)$ MHz]. The magnitude of decoherence is consistently interpreted in terms of the coupling of electrons to piezoelectric acoustic phonons in GaAs.

DOI: 10.1103/PhysRevLett.110.066802 PACS numbers: 73.21.La, 03.67.Lx, 73.63.Kv

Hybridizing different quantum systems is a key step for implementing quantum information processing and quantum communication in scalable systems [1]. For this sake, coherent interaction between different qubits is essential. The photon is a good medium to couple qubits, and the interaction between qubits and photons has been investigated in optical cavity QED experiments [2–4]. The recent technological progress of superconducting qubits has made it possible to couple solid state qubits and on-chip superconducting resonators, forming quantum buses (circuit QED) [5–7]. According to recent theories [8–13], semiconductor quantum dots (QDs) are attractive building blocks for circuit QED because of their high scalability, controllability, and accessibility to the spin degree of freedom. The qubit-resonator coupling strength g and the decoherence rate of the system Γ are two important parameters in such systems: In a strong coupling regime ($g/\Gamma > 1$), a qubit and a photon are no longer independent physical entities but are coupled to form a dressed atom, which can lead to fascinating effects like single-atom lasing [14,15]. Despite pioneering works of semiconductor-based coupled systems [16,17], the realization of vacuum Rabi oscillation has not been reported and coherent interaction in the strong coupling regime has been left to be demonstrated. Here, we report a direct observation of vacuum Rabi splitting in a GaAs/AlGaAs double quantum dot (DQD) based charge qubit coupled with a superconducting coplanar waveguide (CPW) resonator: Coherent oscillation between a single two-level system and single photons has thus been indicated in a semiconductor-based system. Quantitative analysis suggests that the decoherence of the system is dominated by an intrinsic piezoelectric effect in GaAs. This work thus paves the way toward constructing solid-state hybrid devices for quantum information processing and communication.

The device is shown in Figs. 1(a)–1(c) along with its equivalent circuit in Fig. 1(d). A DQD [Fig. 1(c)] is formed in a GaAs/AlGaAs heterostructure crystal containing a two-dimensional electron gas (2DEG) at a 90-nm depth from the surface, where the electron mobility and the sheet electron density are 90 $m^2/V\,s$ and 2.3×10^{15} m^{-2}, respectively, at 4.2 K. A superconducting CPW resonator [Fig. 1(a)] is prepared by depositing a 200-nm-thick aluminum layer on top of the crystal surface where the 2DEG is removed with 50-nm-deep wet etching. The resonator is featured by the resonance frequency $\omega_0/2\pi = 8.3267$ GHz and the decay rate $\kappa/2\pi = 8.0$ MHz at a base temperature ≈ 30 mK (in the condition when the DQD is not formed). The resonator is capacitively coupled to the DQD [C_r; see Figs. 1(c) and 1(d)]. Conductance through the DQD is studied via the standard lock-in technique. The microwave transmitted through the resonator is amplified with a cryogenic amplifier and studied with a vector

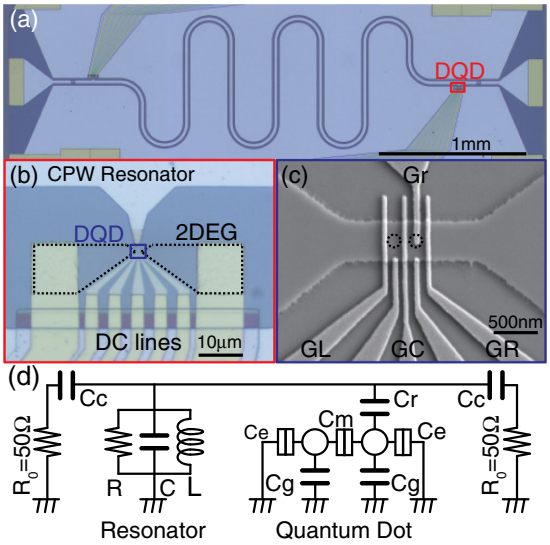

FIG. 1 (color online). (a) Optical microscope image of the coupled DQD-CPW resonator system. The location the where DQD is coupled is marked by the red square, the blown up version of which is shown in (b). (c) It is a scanning electron microscope image of the DQD, defined by biasing metal (NiCr/Au) gates GL (left), GC (center), and GR (right). The right QD is capacitively coupled ($C_r \approx 50$ aF) with gate electrode Gr to the resonator. (d) Equivalent circuit of the device. The two QDs are designed to be nominally equal, except in the presence of Gr. The resonator is weakly coupled at opposite ends to the transmission line through $C_c = 3$ fF.

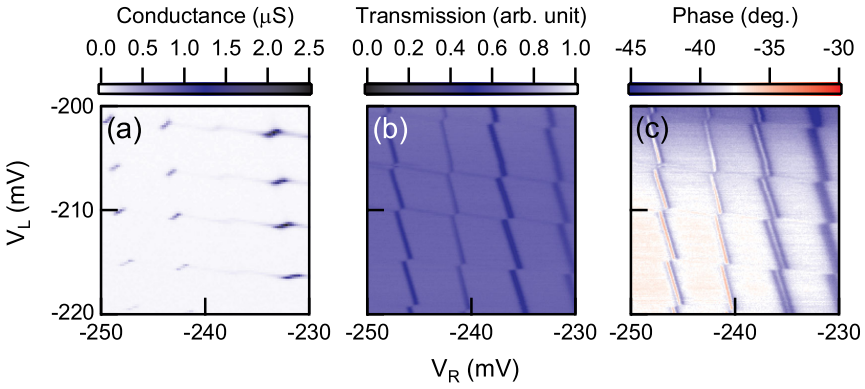

FIG. 2 (color online). Charge stability diagram of the DQD represented on the plane of V_L and V_R, where $V_C = -215$ mV. (a) dc conductance through the DQD, (b) the transmission amplitude, and (c) the phase of the CPW resonator. The microwave frequency is fixed at 8.3267 GHz.

network analyzer [18]. All the measurements are made in a dilution refrigerator at a base temperature below 40 mK. Thermally excited microwave photons in the resonator are completely neglected at 40 mK, with an estimated photon number being less than 5×10^{-5}.

The conductance through the DQD is finite only in the vicinity of charge triple points [Fig. 2(a)] [19]. Because of finite dipole coupling to the resonator, the transmission amplitude and the phase of the resonator exhibit structures along the side edges of the honeycombs [Figs. 2(b) and 2(c)], where the DQD conductance is vanishingly small. Prior to the experiments, photon assisted tunneling (PAT) has been studied for the analysis described later [20]. All the experimental results described below have been carried out with low microwave power such that the PAT is indiscernible. In a simplified model, the resonance frequency of the coupled system is given by $[2\pi\sqrt{L(C + 2C_c + C_{\mathrm{DQD}})}]^{-1}$, where DQD is represented by capacitance C_{DQD}. The amplitude of C_{DQD} is crucially affected by the Coulomb blockade condition between the reservoir and one of the QDs and/or between the QDs because the electrical connection between them thereby turns on or off. The structures in Figs. 2(b) and 2(c) are more distinct along the (vertical) edges of the honeycomb, where the Coulomb blockade between the reservoir and the right QD is lifted. This feature arises from the fact that the "right" QD is coupled to the resonator in our device. (The DQD-resonator coupled system can be quantitatively analyzed in more detail [18].)

The distinct signature of the strong coherent quantum mechanical interaction between the two-level system (DQD) and the microwave photons (resonator) shows up when (i) the microwave power for the resonator is reduced so that the number of photons in the resonator $n < 1$ and (ii) the interdot tunneling is intensified from the level of Fig. 2 by tuning V_C for GC [18]: It manifests itself as two sharp parallel structures in a region between two paired charge triple points, as is shown in Fig. 3(b). Figure 3(a) shows the electrical conductance through the DQD in the vicinity of charge triple points. We find that the transmission amplitude of the resonator [Fig. 3(b)] exhibits remarkably sharp dips along two parallel lines connecting the paired charge triple points: In this region, the interdot Coulomb blockade is lifted and coherent interdot single-electron tunneling takes pace by emitting or absorbing the single microwave photon.

The transmission spectra of the resonator vary as V_L and V_R are scanned along the dashed red line in Fig. 3(b), as is shown in Fig. 4(a), where the horizontal coordinate is given by the (unperturbed) interdot energy difference ε [20]. The spectra show two sharp dip lines. The peak frequency of the spectra exhibits distinct anticrossings, as is shown in Fig. 4(b) [18], and the resonance linewidth increases significantly in the vicinity of the anticrossing points [Fig. 4(c)]. The anticrossings occur exactly at the ε values where the two-level energy splitting, $\Delta = \sqrt{\epsilon^2 + 4t^2}$, equals ω_0 [Fig. 4(d)]. Here, t is the interdot tunnel rate of the DQD estimated to be $t/2\pi \approx 1.5$ GHz in the present experiments [18].

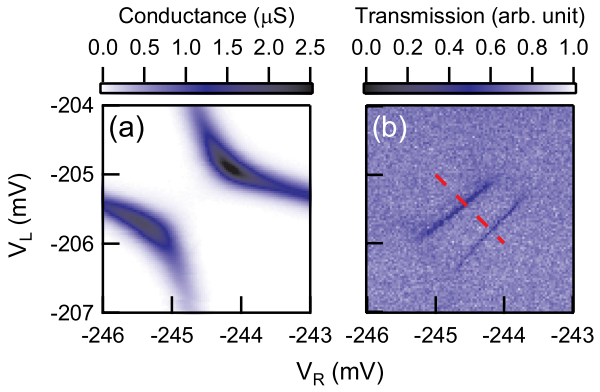

FIG. 3 (color online). (a) The DQD conductance and (b) the resonator transmission amplitude at 8.3267 GHz in the vicinity of charge triple points, with $V_C = -200$ mV.

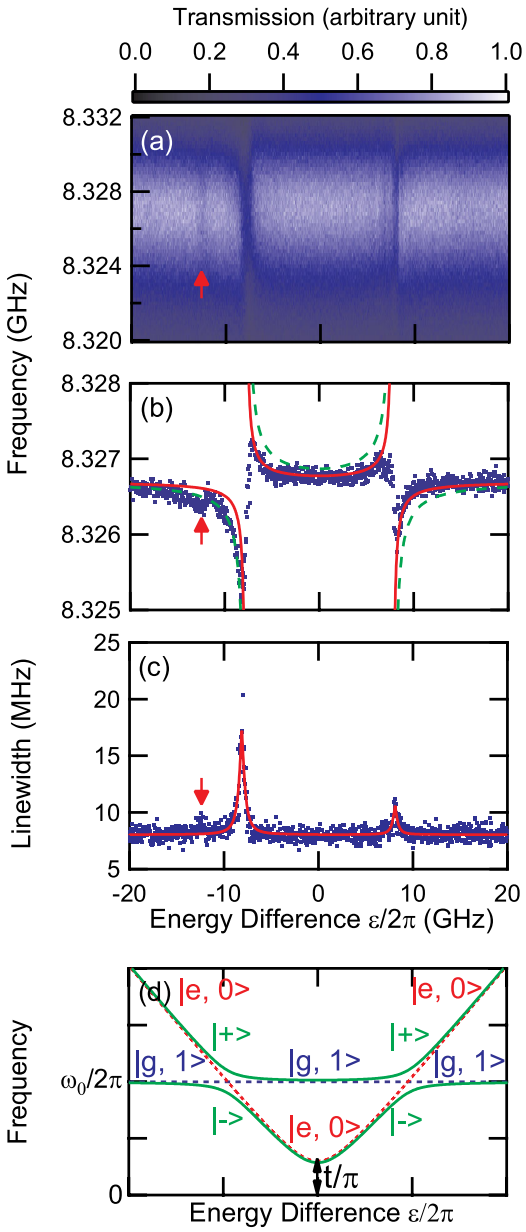

FIG. 4 (color online). (a) Transmission spectra of the resonator as a function of interdot energy difference ϵ. V_L and V_R are scanned along the dashed red line in Fig. 3(b). The gate voltages are converted to the energy difference in frequency units using a conversion constant derived from PAT measurements [20]. (b) The peak position and (c) the linewidth of the transmission spectra. The solid red (dashed green) curve in (b) indicates theoretical values [Eq. (2)], with $g/2\pi = 20(30)$ MHz. (d) Energy diagram of the DQD (thin dashed red curve, $|e, 0\rangle$), the resonator (horizontal dotted blue line, $|g, 1\rangle$) and the coupled system (solid green curves, $|\pm\rangle$). The corresponding quantum states are denoted by the respective colors.

At the anticrossing points, the DQD and the resonator coherently couple via photon exchange. The independent description of the DQD and the resonator is thereby replaced with a dressed atom picture represented by the states, $|\pm\rangle = (|e,0\rangle \pm |g,1\rangle)/\sqrt{2}$ [Fig. 4(d)], where $|g(e), n\rangle$ is the ground (excited) state of the DQD with n photons in the resonator.

The DQD-resonator coupled system is described by

$$\hat{H} = \frac{\hbar\Delta}{2}\hat{\sigma}_z + \hbar\omega_0\left(\hat{a}^\dagger\hat{a} + \frac{1}{2}\right) + \hbar g(\hat{\sigma}^+\hat{a} + \hat{\sigma}^-\hat{a}^\dagger), \quad (1)$$

according to the Jaynes-Cummings model [8]. Here, $\hat{\sigma}_z$, $\hat{\sigma}_+$, and $\hat{\sigma}_-$ are the Pauli operators for the DQD, $\hat{a}$ ($\hat{a}^\dagger$) is the annihilation (creation) operator of a photon and g is the coupling strength between the DQD and the resonator. The resonance frequencies of the coupled system, $\omega_\pm$, are given by

$$\omega_\pm = \frac{\Delta}{2} + \frac{\omega_0}{2} \pm \frac{1}{2}\sqrt{(\Delta - \omega_0)^2 + 4g^2} \quad (2)$$

when $n \ll 1$ [21]. As is shown in Fig. 4(b), the experimental peak frequencies for the right (left) branch are well reproduced by the theoretical curves of Eq. (2) with $g/2\pi = 20(30)$ MHz. We mention that these values of g are consistent with theoretical expectations [18].

The decoherence rate of the system is derived from the experimental linewidth in Fig. 4(c) to be $\Gamma/2\pi = 10(17)$ MHz for the right (left) branch. Hence, the decoherence rate of the DQD is estimated to be $\gamma/2\pi = 12(25)$ MHz for the right (left) branch. [Note that (i) $\Gamma = (\gamma + \kappa)/2$ because the system energy is equally distributed between the DQD and the resonator in vacuum Rabi oscillation and (ii) the decay rate of the resonator has been determined to be $\kappa/2\pi = 8.0$ MHz in independent measurements.] From these values, additional parameters are derived [22]; viz., the number of Rabi oscillation flops $n_{\mathrm{Rabi}} \equiv g/\Gamma = 2g/(\kappa + \gamma) = 1.8(2.0)$, the critical photon number $n_0 \equiv \gamma^2/2g^2 = 0.2(0.3)$, and the critical atom number $N_0 \equiv 2\gamma\kappa/g^2 = 0.5(0.4)$. The physical implication of these numbers is that two flops of vacuum Rabi oscillation are expected ($n_{\mathrm{Rabi}} \approx 2$) and that one photon (atom) is sufficient to bring about saturation in the response of the atom (photon) [$n_0(N_0) < 1$]. We hence conclude that the system is in a strong coupling regime with distinct vacuum Rabi oscillation [23].

The decoherence rate of our DQD, $\gamma/2\pi = 12(25)$ MHz, is a sum of the energy relaxation rate γ_1 and the dephasing rate γ_ϕ; viz., $\gamma = \gamma_1/2 + \gamma_\phi$ [24]. The energy relaxation is primarily dominated by the emission of piezoelectric acoustic phonons in GaAs/AlGaAs DQDs [25,26], the rate of which is estimated to be $\gamma_1/2\pi \approx 8$–40 MHz from the pulsed gate measurements [27]. The fact that the estimated decoherence rate of our DQD, $\gamma/2\pi = 12(25)$ MHz, is not remarkably larger than the intrinsic energy relaxation rate $\gamma_1/2\pi \approx 8$–40 MHz implies that the dephasing rate is small [$\gamma_\phi/2\pi < \gamma/2\pi = 12(25)$ MHz] in our device. In earlier experiments [16], the anticrossing structure was not discerned, probably due to the high dephasing rate $\gamma_\phi \gg g$. The dephasing rate of the gated GaAs/AlGaAs devices is

known to be highly device specific and is supposed to be dominated by the background charge fluctuation [27,28].

The energy loss of the resonator $\kappa/2\pi = 8.0$ MHz occurs through either the photon escape to the external transmission line (coupling loss) or the photon loss inside the resonator (internal loss) [29]. In our device, the coupling capacitance $C_c = 3$ fF is so small that the coupling loss is negligibly small ($\kappa_{\text{ext}}/2\pi = 0.4$ MHz). The internal loss arises from the radiative loss, the metallic loss, and the dielectric loss. In the CPW resonator used here, the radiative loss is small because the resonator width is much smaller than the wavelength and the metallic loss is negligible in our superconducting CPW resonator. The dielectric loss is hence dominant. The decay rate of a CPW is reported to depend on the substrate material, where the order of the rate is such that Si < sapphire < SiN_x < SiO_2 < AlN < MgO [30]. The present authors find that this material-specific feature, along with the absolute decay rates for respective materials, can be consistently ascribed to the piezoelectric effect; that is, oscillating electrical fields generated by CPW resonators are absorbed to excite lattice vibration in the substrate via piezoelectric interaction. From the piezoelectric constant of GaAs $d_{14} = 2.7$ pC/N [31], the decay rate is estimated to be 1.6–16 MHz [18], which roughly explains the experimental value $\kappa/2\pi = 8.0$ MHz.

It is an extremely interesting challenge to realize semiconductor circuit QED devices with a higher coupling-to-decoherence ratio, g/Γ, for implementing highly integrated quantum buses. Since the decoherence is dominated by the intrinsic piezoelectric effect in GaAs, non- or less-piezoactive materials such as Si, SiGe, and carbon-based materials will be highly promising for constructing higher performance semiconductor quantum devices.

In conclusion, we have demonstrated distinct vacuum Rabi splitting in a strongly coupled GaAs DQD and CPW resonator system. The mechanism of decoherence both for the DQD and for the CPW resonator is suggested to be due to the intrinsic piezoelectric effect. The present work not only encourages the further challenge of developing GaAs-based devices but also suggests expanding the effort to less-piezoactive materials.

This work is supported by KAKENHI, Grant-in-Aid No. 22-861. The GaAs/AlGaAs heterostructure crystal is provided by I. Hosako and M. Patrashin at NICT. We thank T. Fujisawa and O. Asterfiev for fruitful discussions.

*toida@thz.c.u-tokyo.ac.jp
†Present address: Department of Applied Physics, University of Tokyo, 7-3-1 Hongo, Bunkyo-ku, Tokyo 113-8656, Japan.

[1] I. Buluta, S. Ashhab, and F. Nori, Rep. Prog. Phys. **74**, 104401 (2011).
[2] C. J. Hood, M. S. Chapman, T. W. Lynn, and H. J. Kimble, Phys. Rev. Lett. **80**, 4157 (1998).
[3] S. Ates, S. M. Ulrich, A. Ulhaq, S. Reitzenstein, A. Löffler, S. Höfling, A. Forchel, and P. Michler, Nat. Photonics **3**, 724 (2009).
[4] D. Englund, A. Majumdar, A. Faraon, M. Toishi, N. Stoltz, P. Petroff, and J. Vučković, Phys. Rev. Lett. **104**, 073904 (2010).
[5] M. A. Sillanpaa, J. I. Park, and R. W. Simmonds, Nature (London) **449**, 438 (2007).
[6] J. Majer, J. M. Chow, J. M. Gambetta, J. Koch, B. R. Johnson, J. A. Schreier, L. Frunzio, D. I. Schuster, A. A. Houck, A. Wallraff, A. Blais, M. H. Devoret, S. M. Girvin, and R. J. Schoelkopf, Nature (London) **449**, 443 (2007).
[7] G. K. Brennen, D. Song, and C. J. Williams, Phys. Rev. A **67**, 050302 (2003).
[8] L. Childress, A. S. Sørensen, and M. D. Lukin, Phys. Rev. A **69**, 042302 (2004).
[9] G.-P. Guo, H. Zhang, Y. Hu, T. Tu, and G.-C. Guo, Phys. Rev. A **78**, 020302 (2008).
[10] Z.-R. Lin, G.-P. Guo, T. Tu, F.-Y. Zhu, and G.-C. Guo, Phys. Rev. Lett. **101**, 230501 (2008).
[11] A. Cottet and T. Kontos, Phys. Rev. Lett. **105**, 160502 (2010).
[12] P.-Q. Jin, M. Marthaler, J. H. Cole, A. Shnirman, and G. Schön, Phys. Rev. B **84**, 035322 (2011).
[13] X. Hu, Y.-x. Liu, and F. Nori, Phys. Rev. B **86**, 035314 (2012).
[14] J. McKeever, A. Boca, A. Boozer, J. Buck, and H. Kimble, Nature (London) **425**, 268 (2003).
[15] O. Astafiev, K. Inomata, A. O. Niskanen, T. Yamamoto, Y. A. Pashkin, Y. Nakamura, and J. S. Tsai, Nature (London) **449**, 588 (2007).
[16] T. Frey, P. J. Leek, M. Beck, A. Blais, T. Ihn, K. Ensslin, and A. Wallraff, Phys. Rev. Lett. **108**, 046807 (2012).
[17] M. R. Delbecq, V. Schmitt, F. D. Parmentier, N. Roch, J. J. Viennot, G. Fève, B. Huard, C. Mora, A. Cottet, and T. Kontos, Phys. Rev. Lett. **107**, 256804 (2011).
[18] See Supplemental Material at http://link.aps.org/supplemental/10.1103/PhysRevLett.110.066802 for detailed descriptions of experimental methods, detailed theoretical analysis of the experimental results, and a discussion on the quality factor of the resonator.
[19] W. G. van der Wiel, S. De Franceschi, J. M. Elzerman, T. Fujisawa, S. Tarucha, and L. P. Kouwenhoven, Rev. Mod. Phys. **75**, 1 (2002).
[20] From the PAT, the conversion ratio between the gate voltage and the frequency (energy) is derived.
[21] When $n > 1$, the nonlinearity of the Jaynes-Cummings ladder appears if the decoherence of the system is low enough. But, it is difficult to see such nonlinearity in our experiment due to decoherence.
[22] *Cavity Quantum Electrodynamics*, edited by P. R. Berman (Academic, Boston, 1994).
[23] The additional small dip indicated by the red arrows in Figs. 4(a)–4(c) is ascribed to the excited state of the DQD.
[24] R. K. Wangsness and F. Bloch, Phys. Rev. **89**, 728 (1953).
[25] T. Fujisawa, T. H. Oosterkamp, W. G. van der Wiel, B. W. Broer, R. Aguado, S. Tarucha, and L. P. Kouwenhoven, Science **282**, 932 (1998).
[26] T. Brandes and B. Kramer, Phys. Rev. Lett. **83**, 3021 (1999).

[27] T. Hayashi, T. Fujisawa, H. D. Cheong, Y. H. Jeong, and Y. Hirayama, Phys. Rev. Lett. **91**, 226804 (2003).
[28] K. D. Petersson, J. R. Petta, H. Lu, and A. C. Gossard, Phys. Rev. Lett. **105**, 246804 (2010).
[29] L. Frunzio, A. Wallraff, D. Schuster, J. Majer, and R. Schoelkopf, IEEE Trans. Appl. Supercond. **15**, 860 (2005).
[30] A. D. O'Connell, M. Ansmann, R. C. Bialczak, M. Hofheinz, N. Katz, E. Lucero, C. McKenney, M. Neeley, H. Wang, E. M. Weig, A. N. Cleland, and J. M. Martinis, Appl. Phys. Lett. **92**, 112903 (2008).
[31] A. Sadao, J. Appl. Phys. **58**, R1 (1985).